

X-682-73-148

PREPRINT

NASA

66252

THE DIFFUSE X-RAY SPECTRUM FROM 14-200 keV AS MEASURED ON OSO-5

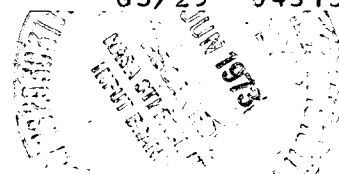
B. R. DENNIS
A. N. SURI
K. J. FROST

(NASA-TM-X-66252) THE DIFFUSE X-RAY
SPECTRUM FROM 14-200 keV AS MEASURED ON
OSO-5 (NASA) 30 p HC \$3.50 CSCL 03B

N73-24815

Unclas
04313

G3/29



GODDARD SPACE FLIGHT CENTER
GREENBELT, MARYLAND

The Diffuse X-Ray Spectrum from 14-200 keV as
Measured on OSO-5

B. R. Dennis, A. N. Suri* and K. J. Frost

Solar Plasmas Branch
Laboratory for Solar Physics
NASA-Goddard Space Flight Center
Greenbelt, Maryland 20771

*NAS-NRC Resident Research Associate
Present address: Physics Department, University of
New Hampshire, Durham, New Hampshire 03824

Abstract

The measurement of the energy spectrum of the diffuse component of the cosmic X-ray flux made on the OSO-5 spacecraft is described. The contributions to the total counting rate of the actively shielded X-ray detector are considered in some detail and the techniques used to eliminate the non-cosmic components are described. Positive values for the cosmic flux are obtained in seven energy channels between 14 and 200 keV and two upper limits are obtained between 200 and 254 keV. The results can be fitted by a power law spectrum of the form:

$$\text{Flux} = (46 \pm 10) E^{-2.08 \pm 0.2} \text{ photons}/(\text{cm}^2 \text{ sec sr keV})$$

A critical comparison is made with the OSO-3 results with the conclusion being that the reported break in the energy spectrum at 40 keV is probably produced by an erroneous correction for the radioactivity induced in the detector on each passage through the intense charged particle fluxes in the South Atlantic Anomaly. If such a break in the spectrum exists at all it cannot be as sharp or as great a change as that reported by Schwartz et al. (1970, Ap. J., 162, 431).

Introduction:

The diffuse cosmic x- and gamma-ray fluxes have been studied extensively over the past few years but despite the large number of measurements, the energy spectrum over the range from 0.25 keV to 10 MeV is not yet well established. Experiments to determine the energy spectrum have been carried out on rockets, balloons and satellites but each method of reaching above the atmosphere has its own peculiar limitations and problems.

The rocket-borne experiments have generally been limited by the short observation time to measuring the spectrum up to energies of only 20 or 30 keV. The rocket data are all consistent with a spectrum of the form

$$I(E) = K E^{-\gamma} \text{ photons}/(\text{cm}^2 \text{ sec sr keV})$$

where the exponent, γ equals 1.4 - 1.7 and the photon energy, E , goes from 1 or 2 keV to 20 or 30 keV. (Seward et al. 1967; Henry et al. 1968; Gorenstein et al. 1969; Green et al. 1969; Toor et al. 1970; Prakasarao et al. 1971; and Henry et al. 1971). Brini et al. (1971) have attempted to extend the range of rocket measurements to 200 keV but with limited statistics.

Measurements at higher energies have been made using balloon-borne detectors where the longer time at altitude allows useful statistics to be accumulated (Rocchia et al. 1967; Rangan et al. 1969; Bleeker and Deerenberg 1970; Davison and Thomas 1971; and Manchanda et al. 1972).

The major difficulty with these measurements lies with the remaining few grams of atmosphere above the detector which prevents cosmic x-rays below about 20 keV from reaching the detector and considerably modifies the spectrum at higher energies. The correction factors which must be applied to the raw data to allow for these effects are difficult to determine and are still being questioned (Makino 1970; Horstman-Moretti 1971; Kasturirangan and Rao 1972). However, the cosmic x-ray spectrum deduced from the data is of the same form as that obtained from rockets but it is apparently somewhat steeper, the exponent power, γ , being between 2.0 and 2.5 in the energy range from 20-220 keV. On the basis of this difference between the spectrum obtained from balloons and from rockets in the two different energy intervals it has been suggested that a break must occur in the spectrum at some intermediate energy.

Just such a break was reported by Schwartz et al. (1970) on the basis of their data from the OSO-3 satellite. For the first time they were able to cover both energy intervals with one instrument, their measurements extending from 7.7 keV to 110 keV. Their results indicated that the exponent γ was 1.7 below 40 keV and 3.1 above 40 keV. Unfortunately, large and uncertain correction factors also had to be applied to the satellite data, particularly at higher energies. Consequently, this result cannot be considered as conclusive evidence for a break in the spectrum.

The principal source of uncertainty in the OSO-3 result arises from the correction factors which must be applied for the effects of the passages through the intense charged particle fluxes in the South Atlantic Anomaly (S.A.A.). Each passage through the trapped radiation produces a residual increase in counting rate of the x-ray detector which slowly decays away after leaving the region of high charged particle fluxes. This effect has been attributed to the production of radio-active isotopes in the x-ray detector and in the satellite itself by interactions of the trapped protons and/or secondary neutrons. The decay products of the isotopes contribute to the total counting rate of the x-ray detector. Thus, before the primary x-ray spectrum can be determined, this detector background must be subtracted.

In the present paper we report the energy spectrum of the diffuse cosmic x-rays from 14-200 keV obtained from the x-ray detector on OSO-5. The detector was similar to that flown on OSO-3 (Schwartz 1969; Hicks et al. 1965), but the larger sensitive area and the increased telemetry available gave over two orders of magnitude improvement in statistics. This has allowed a more detailed understanding of the background corrections to be obtained, and hence we have been able to determine a more reliable diffuse cosmic x-ray spectrum than has previously been possible.

The X-Ray Detector.

The detector used to obtain the results presented in this paper is shown in figure 1. It has been described previously by

Frost et al. (1971) and was designed primarily for studies of solar x-rays (Frost 1969; Frost and Dennis 1971). The x-ray detector consists basically of a CsI(Na) central crystal which is actively shielded by a well-type crystal also of CsI(Na). The central crystal is 0.635 cm thick, has a sensitive area of 70 cm^2 and is viewed from behind by two photomultipliers. The shield crystal has an average wall thickness of 4.4 cm and is viewed by a total of four photomultipliers. The aperture through the shield gives the detector an angular response with a FWHM of 39° and a geometric area x solid-angle factor varying from $34 \text{ cm}^2 \text{ sr}$ at the lowest energies to $47 \text{ cm}^2 \text{ sr}$ at the highest energies detected.

X-ray events are selected when coincident pulses from the two photomultipliers viewing the central crystal occur in the absence of any simultaneous pulse from the photomultipliers viewing the shield crystal. When such an event is detected, the summed pulse from the central crystal is pulse-height analyzed into nine channels: the first channel from 14-28 keV and the other eight channels dividing the energy range from 28-254 keV into approximately equal intervals.

The detector occupies one wheel compartment of the Fifth Orbiting Solar Observatory (OSO-5) which was launched on Jan 22, 1969 into a nearly circular orbit, with a mean altitude of 555 km and an inclination angle of 33° . The detector axis lies along a radial vector of the wheel so that a band of sky about a great circle with its plane perpendicular to the satellite spin axis

is scanned each wheel rotation or approximately every 1.8 sec.

The detailed data collection scheme has been described by Frost et al. (1971). During the satellite day the detector scan circle is divided into 9 approximately equal sectors with one sector centered on the sun. The nine channel pulse-height spectrum plus the dead time is obtained from the solar sector every wheel rotation (\approx every 1.8 sec) and from each non-solar sector for a total of about one second every 100 sec. During the satellite nighttime the nine channel spectrum plus dead time is accumulated for a period of 0.28 sec every 1.28 sec. The detector look direction during the period of data collection can be anywhere in the scan circle and is determined to within the required accuracy of a few degrees from the satellite aspect solution obtained by the Information Processing Division at Goddard Space Flight Center.

In-flight calibration of the energy scale of the detector is obtained by using the 59.4 keV x-rays from the Am^{241} source which is embedded in a plastic scintillator and placed permanently in the aperture as shown in figure 1. Some of these x-rays stop in the central crystal and these events are tagged by the coincident α -particles which produce pulses in the photomultiplier viewing the plastic scintillator. The calibration data have indicated that the gain gradually decreased by 20-30% during the first 300 days in orbit and thereafter remained constant.

The threshold level of the shield has not changed appreciably since launch as indicated by the shield counting rate and the total dead time. It was set at approximately 180 keV before launch and, although we do not have any way of determining its absolute value in orbit, it has probably stayed close to this level.

Evaluation of the Background Corrections

As already indicated the raw data from the x-ray detector on OSO-5 includes not only counts from cosmic x-rays but also counts from many background effects: - charged particles in the radiation belts, charged cosmic ray effects, induced radio - activity, electron precipitations, earth albedo, solar flares, etc. In principle all of these non-cosmic x-ray contributions to the total counting rate can be determined independently and uniquely from their variations with time as the satellite goes around the earth. The rate from the diffuse cosmic x-ray flux on the other hand should stay constant as long as the earth and x-ray point sources are out of the field of view. Thus, if the time varying rates can be determined and subtracted out, the remaining rate should be from the diffuse cosmic x-rays alone.

The first part of the analysis procedure involved the rejection of a large fraction of the available data simply

on the basis of short term increases in counting rate. For this purpose the data were divided into intervals of one orbit or 95 minutes each. This interval was then divided into shorter intervals varying from 1/4 of an orbit down to a single observation. If the rate in any of these periods was greater than four standard deviations above the average rate for the rest of the orbit, then data in that period was rejected. By this method virtually all passages through even the low flux regions of the radiation belts were eliminated. All electron precipitation events and solar flares were also eliminated in this way.

In addition to this rejection of data on the basis of short term increases, data were also rejected under the following conditions:

(i) When the telescope axis was greater than 80° from the zenith at the center of the look interval. This was to remove all effects of the earth in the field of view.

(ii) When the magnetic shell parameter, L, was greater than 1.7 earth radii and the magnetic field was greater than 0.38 gauss. At higher values than these the counting rate was found to be considerably higher than average.

(iii) When the satellite longitude was $60-180^{\circ}$ W or $140-180^{\circ}$ E. The rate was found to be higher in these longitude regions probably because of the electrons which have been observed below the main radiation belts with a similar

longitude variation (Imhof 1971).

(iv) When the interpolated orbit start-longitude was $0-180^{\circ}\text{W}$ or $0-20^{\circ}\text{E}$. (The interpolated orbit start-longitude at any particular time is defined as the orbit start-longitude (the south-to-north equatorial crossing) plus the fraction of the orbit completed multiplied by the change in start-longitude each orbit (24.35°). This parameter was useful in summing many days worth of data since data taken at the same interpolated orbit start-longitude corresponds to approximately the same effective time out of the S.A.A.) The rejection of this large fraction of the data on orbits which passed through the S.A.A. was necessary because of the complicated build-up and decay of the counting rate on these orbits. Also the contributions from the short lived components with decay times less than an hour or so were eliminated in this way.

(v) When any known bright discrete source of x-rays was in the field of view. Also all data taken in the solar sector was rejected.

After the above selection criteria were applied a set of data was obtained which represented the lowest average counting rate of the detector. It was obtained simply by selection on the basis of various parameters and no curve fitting, interpolation or extrapolation was involved. From this set of data we have calculated an energy spectrum assuming

the counts are all from x-rays entering the aperture of the detector. This spectrum is given in table 1 and is shown in figure 4 as the "uncorrected spectrum". It represents an absolute upper limit to the cosmic x-ray spectrum.

The further analysis of the data in an attempt to obtain a more realistic measure of the diffuse spectrum involves assumptions about the origin of the excess rate remaining after passage through the S.A.A. We have assumed that the excess rate observed on leaving the S.A. A. is the result of the decay of the radioactive isotopes produced by proton spallation interactions and possibly also by secondary neutron interactions and capture in the material of the detector and of the surrounding spacecraft. Dyer and Morfill (1971), and Fishman (1972) have shown that protons with energies in excess of 100 MeV produce many different isotopes with half-lives ranging from fractions of seconds up to many years when they are incident on CsI or NaI crystals. As a result, the decay curve of all the spallation products is not an exponential with a single time constant but rather the sum of many exponentials all with different time constants.

A more detailed account of our results on induced radioactivity will be given elsewhere but for the purposes of obtaining the best estimate of the diffuse cosmic x-ray flux we have used an expression of the form given by Barbier (1969)

for the decay in the rate, R , at a time, t , after the irradiation when many different isotopes are formed:

$$R = A/t + C \quad (C)$$

Where A is a constant depending on the intensity of the radiation and C is the counting rate before the irradiation. In our case the exact definition of " t " is somewhat arbitrary because of the many successive irradiations in the S.A.A. but we have set $t = 0$ when the interpolated orbit start longitude = $15^{\circ}E$ to obtain a good fit to the data. In figure 2 we show the decay in counting rates averaged over many days worth of data together with the best fit curve of equation (1).

Clearly, this simple equation leaves much to be desired but it is an approximation which fits the data and gives a means of estimating the contribution of the induced radioactivity to the total detector counting rate.

By using best fit values of A and C in equation 1, we obtained the rates at an interpolated orbit start longitude of $180^{\circ} E$. These were close to the minimum rates observed each day since they were immediately prior to entering the S.A.A. for the first time in each 24-hour period. It was found that these minimum rates were not constant from day to day. Except for the two lowest energy channels, they increased with a time constant of many days. This we interpreted as resulting from'

the build-up of radio-active isotopes with relatively long half-lives. (The rate in the lowest two channels actually decreased after launch but this can be accounted for by the decrease in gain as indicated by the Am^{241} calibration system). Consequently we had to correct the data for this build-up in rate, which was somewhat different in each channel.

In addition to this build-up in rate there was also a systematic variation in rate with the altitude of the satellite in the S.A.A. This was presumably caused by the strong altitude dependence of the proton flux in the lower part of the inner radiation belt. A residual variation of rate with magnetic-shell parameter, L , was also observed. To compensate for these small variations the rates were normalized rather arbitrarily to an L value of 1.0 earth radii and an altitude in the S.A.A. of 540 km. The normalization parameters used are given in table 1.

After these corrections were applied, we fitted the build-up in rates with single or double exponential curves allowing the intensities and time constants to vary to give the best fits. The data did not give good fits to the build-up curve to be expected if equation 1 applied to these long-lived isotopes probably because only a few isotopes were involved. The corrected rates together with the fitted exponential build-up curve for one particular energy channel are shown in figure 3. The form of the build-up curve was chosen on the basis of the data taken from the

time the experiment was first switched on four days after launch to 275 days after launch. Unfortunately, significant build-up may occur in the first four days in orbit but we have no way of estimating the magnitude of this effect from our data. The data in Figure 3 does show some indication of a more rapid build-up in the first ten days in orbit but the scatter of the points is too large to draw any definite conclusions.

Using fitted build-up curves similar to the one shown in Figure 3, we obtained the counting rates extrapolated to the launch day for each energy channel. The final extrapolated rates and the various correction factors used are given in Table 1.

The Diffuse X-Ray Spectrum

The energy spectrum was obtained from the corrected and extrapolated rates by determining factors to convert from counts/sec to photons/(cm² sec sr keV) for each channel using the calculated efficiencies and solid angles. In the case of the two lowest energy channels, because of the uncertainties in the efficiencies, the observed response to the Crab Nebula spectrum was used to determine the conversion factors. The final energy spectrum is given in Table 1 and plotted in Figure 4. The spectrum is best fitted by a power law of the form

$$\text{Flux} = (46 \pm 10) E^{-2.08 \pm 0.2} \text{ photons}/(\text{cm}^2 \text{ sec sr keV})$$

over the energy range from 14 to 200 keV.

The results obtained from OSO-3 by Schwartz et al. (1970) are also shown in figure 4. As can be seen the agreement between the two corrected spectra is excellent while there is a considerable difference between the uncorrected spectra. The reason for the differences between the uncorrected spectra is not clear since, as previously mentioned, the two detectors were very similar. Possible explanations are (i) the higher threshold level on the shield crystal on OSO-3 or (ii) the improved ability to reject data with significantly higher rates as a result of the increased statistics on OSO-5.

The agreement between the two corrected spectra must, however, be considered fortuitous in view of the different correction procedures which were used. In particular, Schwartz (1969) used the following procedures which in the light of the present data on induced radioactivity now seem to be erroneous:

(i) The decay in rate after leaving the S.A.A. was fitted with an exponential curve with a 15-hour half-life, the rationale being that Na^{24} was produced by neutron capture in the NaI central crystal and by (n,α) reactions with the aluminum in the detector and in the surrounding satellite. In contrast, if a single exponential decay curve is used instead of equation 1 to fit the OSO-5 data, a half-life of only ~ 2 hours is obtained.

There seems to be no reason why a 15-hour decay would be observed by the OSO-3 detector and an approximately 2-hour decay by the OSO-5 detector. It is unlikely that sufficient Na^{24} would be produced to dominate the spectrum over the other spallation products in either of the two major components which differed significantly between the two detectors: the NaI central crystal on OSO-3 vs CsI on OSO-5 and the greater quantity of aluminum surrounding the central crystal and the shield crystal on the OSO-3 detector. The most likely explanation of the 15-hour fit to the OSO-3 data comes from the method of selection of the data itself. The counting rates after every passage through the S.A.A. was used in the fitting procedure whereas only the rates after the last passage through the S.A.A. in any particular 24-hour period should be used. Because of the contribution from longer lived isotopes, there is a build-up in rate after each successive passage through the S.A.A. If data from all of the five or six orbits per day when the satellite passes through the S.A.A. are used, then the average rate for the first 90 minutes after leaving the S.A.A. will be artificially lowered and a least squares fit will give a time constant which is too long.

(ii) The observed build-up in rate in the first two weeks after the launch of OSO-3 was not used to extrapolate the rate vs. time curve back to the launch day. The increase in the shield threshold level during this period could account for some of this increase in rate but there seems no reason to suppose that the build-up in rate after launch observed on

OSO-5 would not also be present on OSO-3.

In addition to the above the following significant differences exist between the OSO-3 and the OSO-5 analysis procedure:

(i) The improved statistics on OSO-5 allowed the elimination of data on the basis of small but significant short-term increases in the counting rate.

(ii) The variation of rate with geographic longitude observed on OSO-5 was not detected on OSO-3. However, the elimination of the longitude intervals when the rate was significantly higher gives less than a 10-20% reduction in the average rate and this was probably offset to some extent by the rejection of data in the electron loss cone in the OSO-3 analysis.

(iii) No variation of aperture with energy was included in the OSO-3 analysis (Schwartz 1971). The effective aperture varies by as much as 40% over the energy range as a result of the absorption of the aluminum housing. Including this variation in the analysis would raise the spectrum at the low energy end although the reported evidence for a break in the spectrum is not removed by this correction alone.

Recently Dyer (1972) has suggested on the basis of his ground-based data on induced radioactivity that the build-up in rate after launch cannot be adequately fitted by a single or a double exponential curve. If this is the case, the

data points above 100 keV would be lowered and in fact the positive detection of the diffuse cosmic x-ray flux at these energies would be brought into question.

In this connection it should be made clear that the only evidence that the spectrum obtained below 100 keV is of cosmic origin and is not due to a residual constant background from an unknown cause lies in the difference between the rates when the earth is in the field of view and out of the field of view. These differences represent lower limits to the possible cosmic component and they are shown in figure 4 for two different energy channels. Above 100 keV the earth becomes as bright as the sky and hence no lower limit can be obtained in this way.

In fact there is evidence that some fraction of the data used to obtain the corrected spectrum does contain additional background contributions. Statistically significant but not systematic variations are observed in this data as can be seen in figure 3.

Conclusion

After a long and exhaustive series of corrections, interpolations and extrapolations we arrive at a spectrum which can be fitted with a power law which is probably somewhat steeper than $E^{-2.0}$ from 14 keV to 200 keV. Although there are many possibilities for error in this analysis and the final result is far from certain, it seems difficult to see how the

spectrum could be much flatter than $E^{-2.0}$ since the uncertainties would tend to make the spectrum even steeper. Leakage through the shield and back scattering into the central crystal would tend to increase the higher energy rates. Also the uncertainties in extrapolating the rates to the launch date could possibly result in overestimating the rate, especially in the high energy channels.

Thus, while the matter is by no means resolved, our results are consistent with the critical analysis of all the available data made by Kasturirangan and Rao (1972), Dyer et al. (1972), and by Brini et al. (1971) in which a single power law spectrum is found to be capable of fitting the data from 1 keV - 1 MeV. However, the uncertainties are such that a break in the spectrum near 40 keV cannot be precluded, although if it exists at all, it is probably not as sharp or as great a change as that suggested by Schwartz et al. (1970).

Acknowledgements

The X-ray detector and associated electronics were built in the Solar Physics Branch at Goddard Space Flight Center. Mr. J. Thornwall was responsible for the initial electronic design while Mr. R. Lencho completed the design work and carried out all the final testing and last minute modifications. Mr. F. Hallberg and Mr. E. Nyberg contributed extensively to the construction and packaging of the electronics and Mrs. Carol Nash assisted with the fabrication. Mr. A. Huffman handled the potting of all the photomultipliers. The mechanical design was done by Mr. George Dietz. Data analysis was carried out with programming contributions from Mrs. A. W. Anderson and dogged computer feeding by Mr. R. McColm.

Finally, we are indebted to all the people in the OSO Project Office and at BBRC who helped make OSO-5 such a successful satellite. Some of this work was carried out while two of us (B. R. Dennis and A. N. Suri) were NAS/NRC fellows at GSFC.

In addition we are grateful to Dr. Daniel Schwartz for his frank and open discussions of the OSO-3 data while he was at GSFC.

REFERENCES

- Barbier, M. 1969, Induced Radioactivity (Amsterdam: North-Holland Publishing Co.), p. 29.
- Bleeker, J.A.M., and Deerenberg, A. J. M. 1970, Ap. J., 159, 215.
- Boldt, E. A., Desai, U. D., and Holt, S. S. 1969, Ap. J., 156, 427.
- Brini, D., Fuligni, F., and Horstman-Moretti, E. 1971, Il Nuovo Cimento, 6B, 68.
- Davison, P. J. N., and Thomas, R. M. 1971, Nature Phys. Sci., 233, 27.
- Dyer, C. S. 1972, Unpublished paper presented at the Gamma Ray Local Production and Shielding Conference, Durham, New Hampshire.
- Dyer, C. S., Engel, A. R., and Quenby, J. J. 1972, presented at COSPAR meeting, Madrid, Spain.
- Dyer, C. S., and Morfill, G. E. 1971, Astrophys. and Space Sci., 14, 243.
- Fishman, G. J. 1972, Ap. J., 171, 163: also Fishman, G. J. 1972, Proton-Induced Radioactivity in NaI (Tl) Scintillation Detectors, Summary Report SE-SSL-1497 (Huntsville, Ala.: Teledyne Brown Engineering).
- Frost, K. J. 1969, Ap. J. (Letters), 158, L159.
- Frost, K. J. and Dennis, B. R., and Lencho, R. J. 1971, New Techniques in Astronomy, Proc. I.A.U. Symp. 41, 185.

- Gorenstein, P., Kellogg, E. M., and Gursky, H. 1969, Ap. J.,
156, 315.
- Green, D. W., Wilson, B. G., and Baxter, A. J. 1969, Space
Research IV (Amsterdam:North Holland Publishing Co.)
p. 222.
- Henry, R. C., Fritz, G., Meekins, J. F., Friedman, H. and
Bryam, E. T. 1968, Ap. J. (Letters), 153, L11.
- Henry, R. C., Fritz, G., Meekins, J. F., Chubb, T., and
Friedman, H. 1971, Ap. J. (Letters), 163, L73.
- Hicks, D. B., Reid, L., Jr., and Peterson, L. E. 1965, IEEE
Trans. Nucl. Sci., NS-12, 64.
- Horstman, H., and Horstman-Moretti, E. 1971, Nature Phys. Sci.,
229, 148.
- Imhof, W. L. 1971, Models of the Trapped Radiation Environment
VII, NASA SP-3024, p. 3.
- Kasturirangan, K., and Rao, U. R. 1972, Astrophys. and Space
Sci., 15, 161.
- Makino, F. 1970, Astrophys. and Space Sci., 8, 251.
- Manchanda, R. K., Biswas, S., Agrawal, P. C., Gakhale, G. S.,
Iyengar, V. S., Kunte, P. K. and Sreekantan, B. V. 1972,
Astrophys. and Space Sci., 15, 272.
- Prakasarao, A. S., Sharma, D. P., Jayanthi, U. B., and Rao, U.
1971, Astrophys. and Space Sci., 10, 150.
- Rangan, K. K., Bhavsar, P. D., and Nerurkar, N. W. 1969,
J. G. R., 74, 5139.

- Rocchia, R., Rothenflug, R., Boclet, Dr., Ducros, G. and
Lebeyrie, J. 1967, Space Research VII (Amsterdam:North-
Holland Publishing Co.), p. 1329.
- Seward, F., Chodil, G., Mark, H., Swift, C., and Toor, A.
1967, Ap. J., 150, 845.
- Schwartz, D. A. 1969, Ph.D. Thesis, Univ. of California at
San Diego.
- Schwartz, D. A. 1971, Private Communication.
- Schwartz, D. A., Hudson, H. S., and Peterson, L. E. 1970,
Ap. J., 162, 431.
- Toor, A., Seward, F. D., Cathey, L. R., and Kunkel, W. E.
1970, Ap. J., 160, 209.

Table 1

Steps made in the data analysis to obtain the spectrum of the diffuse
cosmic x-ray component from the observed counting rates

Energy Levels (KeV)	<u>14</u> 28	<u>28</u> 55	<u>55</u> 82	<u>82</u> 111	<u>111</u> 141	<u>141</u> 168	<u>168</u> 200	<u>200</u> 225	<u>225</u> 254
Observed rates for selected data (counts/sec)	.66	13.40	7.5	5.8	4.8	4.3	3.7	2.9	2.1
Conversion Factors (counts/sec/photons cm ² sec sr keV)	8.4	674	997	1155	1183	973	1016	697	719
Uncorrected Fluxes x 10 ³ (photons/cm ² sec sr keV)	78	19.9	7.5	5.0	4.1	4.4	3.6	4.1	2.9
<i>ll</i> Average counting rates at minimum level in 24-hour period (counts/sec)	.60	12.7	7.1	5.1	3.9	3.3	2.8	2.2	1.6
Variation with Magnetic shell parameter, L. (counts/sec earth radii)	-	.92	.20	.31	.28	.34	.35	.30	.25
Variation with altitude in the S.A.A. (counts/sec 10 ³ km)	4	40	10	16	20	18	17	12	8
Rates extrapolated to launch (counts/sec)	.75	12.6	5.9	4.2	2.29	1.4	.8	.9	.9
Corrected fluxes x 10 ³ (photons/cm ² sec sr keV)	89.3 ±8.7	18.6 ±1.6	5.9 ±.5	3.6 ±.2	1.9 ±.2	1.5 ±.3	.8 ±.3	≤1.3	≤1.2

FIGURE CAPTIONS

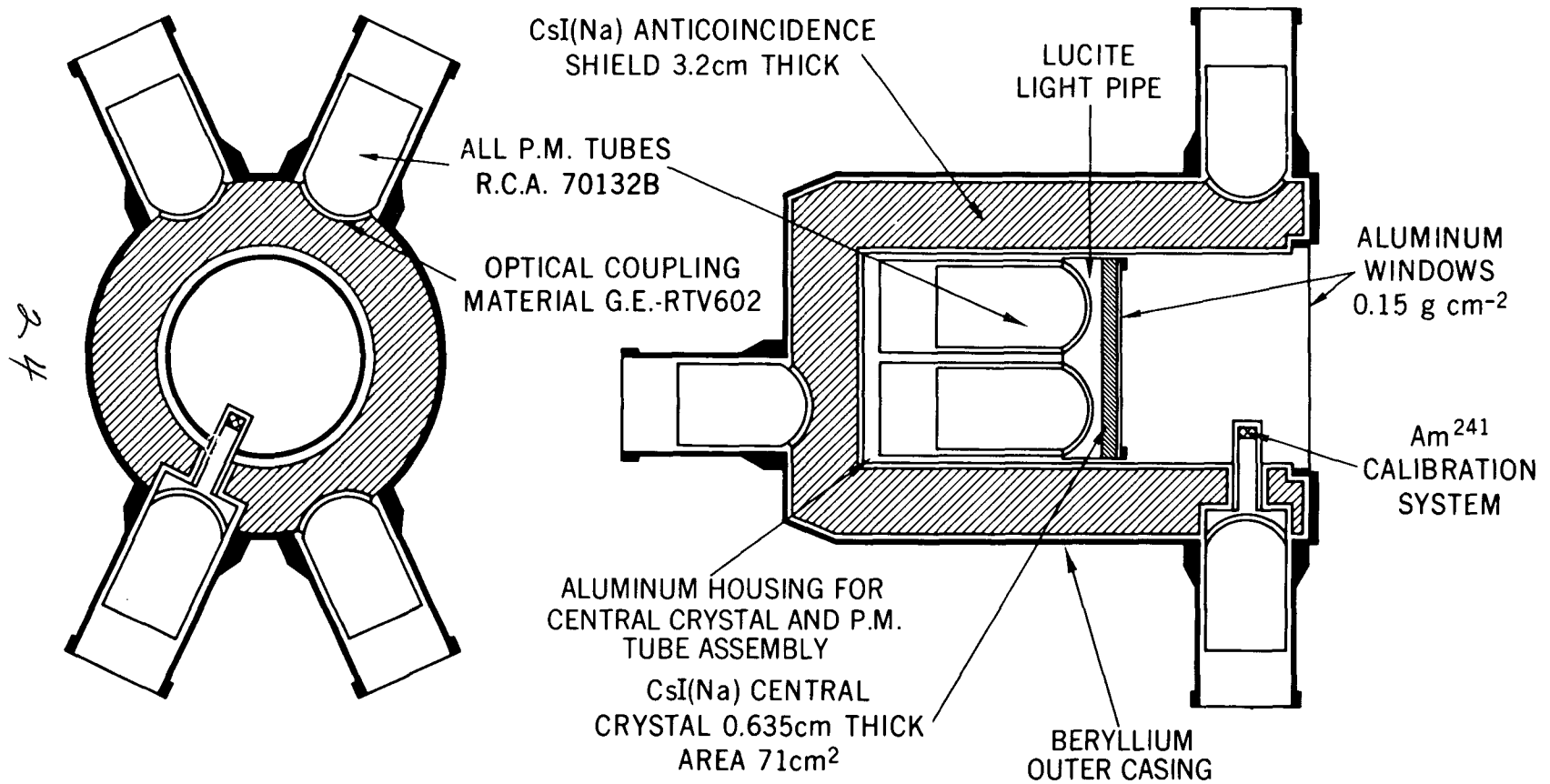
Figure 1. Cross-sectional view of the X-ray detector

Figure 2. The average decay in the counting rate in one energy channel after leaving the S. A. A. for the last time in a 24-hour period. Several days worth of data have been average using the interpolated orbit start-longitude to normalize the time-scale for each day (see text for explanation of the interpolated orbit start-longitude) with the zero defined as the time at which the interpolated orbit start-longitude is 15°E .

Figure 3. The build-up in counting rate for one energy channel after the launch of the satellite. The points are the minimum rates observed each day obtained from interpolated orbit-start longitudes of 180°E after corrections for the variation of rate with the magnetic shell parameter, L , and with the altitude of the satellite in the S. A. A. The typical standard deviation of the data points is ≈ 0.1 counts/sec.

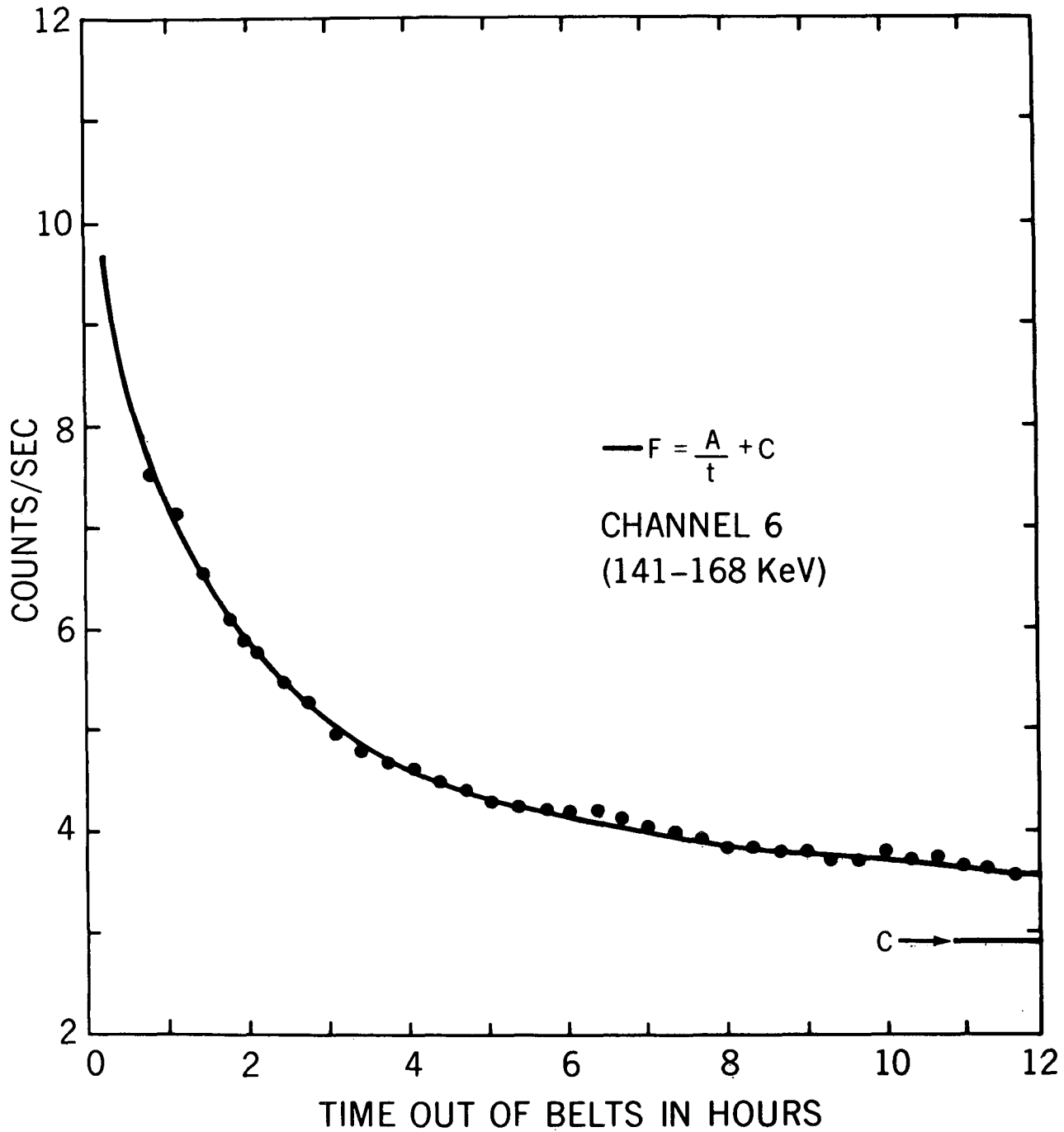
Figure 4. A comparison of the X-ray spectra obtained from OSO-3 and from OSO-5. The corrections applied to the OSO-5 data are described in the text. The line is a power law fit to the corrected OSO-5 data and is of the form Intensity = $46 E^{-2.08}$ photons/cm² sec sr keV.

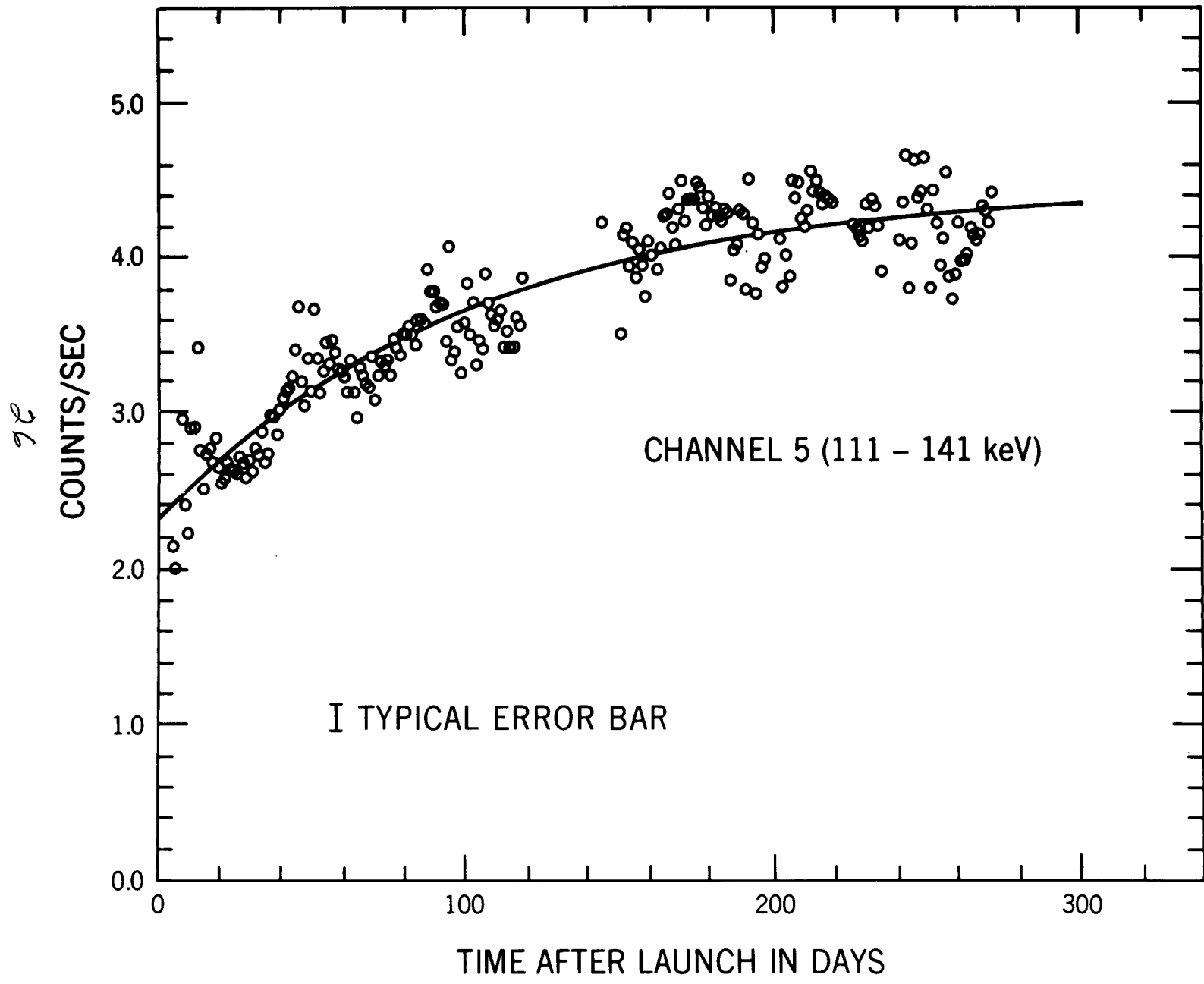
OSO-5 15-250 KEV X-RAY DETECTOR



0 2 4 6
SCALE IN INCHES

DECAY OF RATE AFTER LEAVING RADIATION BELT





SPECTRUM OF DIFFUSE COSMIC X - RAYS

